

# Brain and spinal cord abnormalities in multiple sclerosis

## Correlation between MRI parameters, clinical subtypes and symptoms

G. J. Lycklama à Nijeholt,<sup>1,2</sup> M. A. A. van Walderveen,<sup>1,2</sup> J. A. Castelijns,<sup>1,2</sup> J. H. T. M. van Waesberghe,<sup>1,2</sup> C. Polman,<sup>1,3</sup> P. Scheltens,<sup>1,3</sup> P. F. W. M. Rosier,<sup>4</sup> P. J. H. Jongen<sup>5</sup> and F. Barkhof<sup>1,2</sup>

<sup>1</sup>Dutch MRI Center for MS Research, Departments of <sup>2</sup>Radiology and <sup>3</sup>Neurology, Vrije Universiteit Hospital, Amsterdam and the Departments of <sup>4</sup>Urology and <sup>5</sup>Neurology, Academic Hospital, Radboud, Nijmegen, The Netherlands

Correspondence to: Dr G. J. Lycklama à Nijeholt, Department of Radiology, Vrije Universiteit Hospital, De Boelelaan 1117, 1081 HV Amsterdam, The Netherlands

### Summary

We investigated various magnetic resonance MRI parameters for both brain and spinal cord to see if any improved the clinicoradiological correlation in multiple sclerosis. Ninety-one multiple sclerosis patients (28 relapsing–remitting, 32 secondary progressive and 31 primary progressive) were imaged using conventional T<sub>1</sub>, proton density- and T<sub>2</sub>-weighted MRI of the brain and spinal cord. Focal brain and spinal cord lesion load was scored, as were diffuse signal abnormalities, brain ventricular volume and spinal cord cross-sectional area. Clinical measures included the expanded disability status scale (EDSS), the functional systems score and a dedicated urology complaint questionnaire. Secondary progressive patients differed from relapsing–remitting and primary progressive patients by a larger number of hypointense T<sub>1</sub> lesions in the brain, ventricular enlargement and spinal cord atrophy. Primary progressive patients more often had diffuse abnormalities in the brain and/or spinal cord than did relapsing–remitting and secondary progressive patients. In the entire study

population, EDSS correlated with both brain and spinal cord MRI parameters, which were independent. The urological complaint score correlated only with spinal cord MRI parameters. In relapsing–remitting and secondary progressive multiple sclerosis, the correlation between MRI and clinical parameters was better than in the entire population. In this subgroup EDSS variance could be explained best by T<sub>1</sub> brain lesion load, ventricle volume and spinal cord cross-sectional area. In the primary progressive subgroup the clinicoradiological correlation was weak for brain parameters but was present between spinal cord symptoms and spinal cord MRI parameters. In conclusion, the different brain and spinal cord MRI parameters currently available revealed considerable heterogeneity between clinical subtypes of multiple sclerosis. In relapsing–remitting and secondary progressive multiple sclerosis both brain and spinal cord MRI may provide a tool for monitoring patients, while in primary progressive multiple sclerosis the clinicoradiological correlation is weak for brain imaging.

**Keywords:** multiple sclerosis; MRI; spinal cord; clinicoradiological correlation

**Abbreviations:** DTPA = diethylene triamine pentaacetic acid; EDSS = expanded disability status scale; FSS = functional systems score; TE = echo time; TR = repetition time

### Introduction

Because of the high sensitivity of conventional T<sub>2</sub>-weighted MRI for depicting focal lesions in the brain of multiple sclerosis patients, this technique may provide an objective tool for disease monitoring (Miller *et al.*, 1996).

Disappointingly, the correlation between the number of focal brain lesions and disability measures like the expanded disability status scale (EDSS) is weak (Filippi *et al.*, 1995b), limiting the use of MRI for follow-up of patients. A reason

for this clinoradiological paradox may be that brain lesions are sometimes located in clinically silent areas. Spinal cord lesions more often cause symptoms than do brain lesions (Kidd *et al.*, 1996; Thorpe *et al.*, 1996). However, when combining lesions of both brain and spinal cord, the correlation with EDSS remains weak (Kidd *et al.*, 1993). This may be caused by lack of histological specificity of conventional T<sub>2</sub>-weighted MRI. T<sub>1</sub>-weighted MRI seems to be more specific than T<sub>2</sub>-weighted MRI for detecting clinically relevant lesions (van Walderveen *et al.*, 1995; Truyen *et al.*, 1996).

Another contributor to the clinoradiological paradox in multiple sclerosis may be underestimation of the disease burden, since, apart from focal lesions, generalized changes may develop in normal-appearing white matter of the brain (Loevner *et al.*, 1995; Gasperini *et al.*, 1996). Recently, generalized involvement was also suggested in the spinal cord (Lycklama à Nijeholt *et al.*, 1997). The occurrence of brain (Aschoff *et al.*, 1984; Losseff *et al.*, 1996b) and spinal cord (Kidd *et al.*, 1993; Filippi *et al.*, 1994; Losseff *et al.*, 1996a; Lycklama à Nijeholt *et al.*, 1997) atrophy further supports the concept of generalized multiple sclerosis involvement.

Clinical subtypes of multiple sclerosis differ considerably regarding MRI findings, which influences the relationship between disability and MRI. Relapsing–remitting multiple sclerosis is characterized by the presence of active lesions, seen as a high number of gadolinium-DTPA enhancing lesions (Thorpe *et al.*, 1996). Secondary progressive multiple sclerosis is associated with the presence of large confluent hyperintense brain lesions on T<sub>2</sub>-weighted MRIs (Thompson *et al.*, 1991). Further, in secondary progressive multiple sclerosis these lesions may partly appear as hypointense on T<sub>1</sub>-weighted MRIs (van Walderveen *et al.*, 1995). Primary progressive multiple sclerosis patients have relatively few brain lesions, which are small, despite frequent severe disability (Thompson *et al.*, 1990, 1991). Secondary progressive and primary progressive multiple sclerosis patients may have cervical cord atrophy and, especially in primary progressive multiple sclerosis, diffuse signal changes of the spinal cord (Kidd *et al.*, 1993; Filippi *et al.*, 1996; Lycklama à Nijeholt *et al.*, 1997).

A large study combining various brain and spinal cord MRI parameters in all three subtypes of multiple sclerosis has not yet been performed. Therefore, we performed such a study in order to study (i) relationships between various MRI parameters, and (ii) the correlation between combined MRI findings and clinical parameters.

## Patients and methods

Ninety-one patients (28 relapsing–remitting, 32 secondary progressive and 31 primary progressive) fulfilling the diagnosis of clinically definite multiple sclerosis were recruited from the out-patient clinic of the department of neurology of our hospital. Each patient gave informed consent

after the procedures had been explained. The study was approved by the institutional review board of the Vrije Universiteit Hospital, Amsterdam and the Radboud Academic Hospital, Nijmegen, The Netherlands, in accordance with the Helsinki declaration.

Patients were examined by one neurologist, who was unaware of the MRI appearance. Disability was assessed using the EDSS (Kurtzke, 1983) and the functional systems scale (FSS) (Kurtzke, 1961). The amount and type of urological complaints were scored using a 15-point urological questionnaire, ranging from 0 to 27 (Appendix 1).

## MRI

MRI was performed at 1.0 T (Magnetom Impact; Siemens, Erlangen, Germany), immediately after administration of gadolinium-DTPA (0.1 mmol/kg). MRI of the brain consisted of proton density- and T<sub>2</sub>-weighted conventional spin echo [2300/45,90/1 (TR/TE excitations)] and T<sub>1</sub>-weighted conventional spin echo (600/15/2) pulse sequences. Twenty-one axial slices were obtained, with an in-plane resolution of ~1 mm, a slice thickness of 5 mm and an interslice gap of 0.5 mm. MRI of the spinal cord was performed using a spinal phased array coil. Sagittal slices (slice thickness 3 mm, interslice gap 0.3 mm) were acquired using cardiac-triggered conventional spin echo (2200/20,80/1; proton density- and T<sub>2</sub>-weighted) and T<sub>1</sub>-weighted spin echo (550/15/2). The field of view was 240×480 mm and the imaging matrix was 256×512, yielding pixels of 0.94 mm<sup>2</sup>. One 5 mm thick slice was acquired perpendicular to the spinal cord at C2 level, using T<sub>2</sub>\*-weighted gradient echo [620/20/20E/4 (TR/TE/flip angle/excitations)]. In-plane resolution was 0.90 mm for this sequence. Total MRI acquisition time was ~1 h.

## Analysis

Focal lesions in the brain and spinal cord were defined as areas of hypointensity (T<sub>1</sub>-weighted images) or hyper-intensity (T<sub>2</sub>-weighted images) sharply demarcated from surrounding tissue. Focal lesions were counted and marked on hard copies by one experienced reader, who was blinded to clinical data. In addition, brain and spinal cord MRIs were scored for the presence of diffuse abnormalities, defined as poorly demarcated high signal areas as seen on both proton density and T<sub>2</sub> images. Scoring was performed by two readers by consensus. In the brain the presence or absence of diffuse abnormalities was scored, and in the spinal cord the length of diffuse abnormalities, expressed as the number of vertebral segments involved, was scored.

The volume of previously identified focal brain lesions was calculated on a workstation (Sun, Mountainview, Calif., USA) using home-developed semiautomated local thresholding software, by a single observer. The T<sub>1</sub> and T<sub>2</sub> lesion volumes (cm<sup>3</sup>) were calculated by adding the areas of all lesions and multiplying by slice thickness and interslice distance.

The area of brain ventricles was measured on T<sub>1</sub>-weighted MRIs, using local thresholding software. Total brain ventricular area was measured on all slices showing CSF within the ventricles. Ventricle volume (cm<sup>3</sup>) was calculated by multiplying total ventricle area by slice thickness and interslice distance. The ventricle volume calculation was performed twice by the same observer with an interval of at least 1 month, and the average of these two measurements was used.

The cross-sectional area of the spinal cord (mm<sup>2</sup>) was calculated on the axial T<sub>2</sub>\*-weighted MRI at level C2 by one observer using local thresholding. Cross-sectional area calculation was performed twice with an interval of at least 1 month, and the average of two measurements was used.

Contrast measurements were performed on proton density-weighted brain images. Regions of interest were placed in the periventricular white matter (not in focal lesions) and in adjoining CSF of lateral ventricles by a single observer who was unaware of clinical data. If a diffuse periventricular signal increase was present, the region of interest was directed within such an area. Contrast ratios were calculated by dividing the signal intensity of brain tissue by the signal intensity of CSF.

Comparisons between subtypes of multiple sclerosis and between different types of MRI abnormalities were made using Student's *t* test for normally distributed data, while the Mann-Whitney *U* test was used for non-parametric data. Intra-observer variability was expressed as the mean of the absolute difference between two measurements divided by the mean of two measurements. Correlations were calculated as Spearman's rank correlation coefficient. Multiple regression analysis (forward) was performed using EDSS and the urology score as the dependent variable and several brain and spinal cord MRI parameters as independent factors. For correlation coefficients and multiple regression analysis, a *P* value of less than 0.01 was considered statistically significant, while a value between 0.01 and 0.05 was considered a trend.

## Results

Clinical data for each clinical subgroup are listed in Table 1. Median age of both secondary progressive and primary progressive patients was higher than that of relapsing-remitting patients, and disease duration was longer. Further, the median EDSS of secondary progressive and primary progressive patients was higher than that of relapsing-remitting multiple sclerosis patients. Scores for symptoms associated with spinal cord abnormalities (FSS subscores for pyramidal, sensory and bowel/bladder symptoms) were significantly higher for secondary progressive and primary progressive than for relapsing-remitting multiple sclerosis. Secondary progressive and primary progressive multiple sclerosis patients had higher urology complaints scores than did relapsing-remitting patients.

Data regarding MRI abnormalities, classified by multiple

**Table 1** Clinical data classified by clinical subtype

	RR (n = 28)	SP (n = 32)	PP (n = 31)
Age (years)	35 (25–57)	46 (30–65)	45 (20–69)
Male : female ratio	10 : 18	13 : 19	14 : 17
Disease duration (years)	5 (1–30)	9 (1–40)	6 (1–24)
EDSS (0–10)	1 (0–4.5)	4.75 (2–6.5)*	4.5 (2–6)*
FSS subscores			
Visual (0–5)	0 (0–4)	0 (0–4)	0 (0–2)
Mental (0–5)	0 (0–1)	0 (0–3)	0 (0–2)
Brainstem (0–5)	0 (0–2)	0 (0–2)	0 (0–4)
Cerebellar (0–5)	0 (0–3)	0 (0–3)	0 (0–4)
Pyramidal (0–5)	1 (0–4)	3 (0–5)*	3 (1–5)*
Sensory (0–5)	0 (0–2)	1 (0–4)*	1 (0–4)*
Bowel/bladder (0–5)	1 (0–4)	1.5 (0–4)*	2 (0–3)*
Urology score			
Urological questionnaire (0–27)	3 (0–14)	9 (0–17)*	8.5 (0–17)*

All values are expressed as median (range). Statistics: Mann-Whitney *U* test. \**P* < 0.001, PP and SP versus RR. RR = relapsing-remitting; SP = secondary progressive; PP = primary progressive; EDSS = expanded disability status scale; FSS = functional systems score.

sclerosis subtypes, are listed in Table 2. Intra-observer variability of the measurements of ventricular volume and spinal cord cross-sectional area were 6 and 3%, respectively. Similarly to clinical findings, considerable differences were present between various multiple sclerosis subtypes regarding brain MRI abnormalities (Figs 1–3). Secondary progressive multiple sclerosis patients had significantly higher focal T<sub>1</sub> and T<sub>2</sub> lesion load than did relapsing-remitting and primary progressive multiple sclerosis patients, while the latter two groups did not differ significantly regarding T<sub>1</sub> or T<sub>2</sub> lesion load. The ratio between T<sub>1</sub> and T<sub>2</sub> lesion load was higher in secondary progressive and primary progressive multiple sclerosis patients than in relapsing-remitting multiple sclerosis patients (Table 2). The number of gadolinium enhancing brain lesions was slightly, but not significantly, higher in the relapsing-remitting and secondary progressive groups than in the primary progressive group. Diffuse brain abnormalities were found significantly more often in the primary progressive multiple sclerosis group (nine of 31 patients) than in both the relapsing-remitting (three of 28 patients) group and the secondary progressive group (four of 32 patients;  $\chi^2 = 4.8$ ; *P* < 0.05). Diffuse brain abnormalities were found mostly in the parietal periventricular white matter (Fig. 3). The median contrast ratio between the brain white matter and CSF was higher in primary progressive patients than in both relapsing-remitting and secondary progressive patients (Table 2).

Focal spinal T<sub>1</sub> lesions were not detected in any clinical subgroup. No significant differences were found in the

**Table 2** MRI abnormalities classified by multiple sclerosis subtypes

	RR (n = 28)	SP (n = 32)	PP (n = 31)
<b>Brain</b>			
T <sub>2</sub> focal lesion load (cm <sup>3</sup> )	4.1 (0–23.6)	11.0 (0.1–49.2) <sup>†</sup>	3.2 (0.4–32.1)
T <sub>1</sub> focal lesion load (cm <sup>3</sup> )	0.3 (0–3.4)	2.0 (0–27.2) <sup>†</sup>	0.3 (0–11.5)
T <sub>1</sub> : T <sub>2</sub> load ratio	0.09 (0–0.45)	0.17 (0–0.71)	0.12 (0–0.54)
No. of patients with enhancing lesions (%)	10 (36%)	9 (28%)	7 (23%)
No. of patients with diffuse abnormalities (%)	3 (11%)	4 (13%)	9 (29%)
Ventricle volume (cm <sup>3</sup> )	22.3 (10.1–42.3)	31.9 (15.3–88.9) <sup>†</sup>	21.3 (9.2–61.7)
Brain WM : CSF contrast ratio	0.89 (0.79–1.0)	0.89 (0.81–1.25)	0.92 (0.83–1.11) <sup>§</sup>
<b>Spinal cord</b>			
T <sub>2</sub> focal lesion load	2.25 (0–6.5)	2.0 (0–9)	2.4 (0–13)
T <sub>1</sub> focal lesion load	0	0	0
No. of patients with enhancing lesions (%)	0	2 (6%)	0
No. of segments showing diffuse abnormalities (%)	0 (0–19)	0 (0–19)	15 (0–19) <sup>§</sup>
No. of patients with diffuse abnormalities (%)	6 (21%)	10 (31%)	19 (61%) <sup>¶</sup>
CSA (mm <sup>2</sup> )	77.5 (49–91.5) <sup>‡</sup>	67 (53–96)	72 (57.5–96)

All values are expressed as median (range) or median (percentage). Statistics: Mann–Whitney *U* test and  $\chi^2$  test. Note that in three of the RR and in one PP multiple sclerosis patient a T<sub>1</sub> : T<sub>2</sub> lesion load ratio of the brain could not be calculated because the T<sub>2</sub> lesion load was 0. CSA = cross-sectional area; WM = white matter; CSF = cerebrospinal fluid. <sup>†</sup>*P* < 0.01, SP versus RR and PP; <sup>‡</sup>*P* < 0.01, RR versus SP; <sup>§</sup>*P* < 0.01, PP versus RR and SP; <sup>¶</sup> $\chi^2 = 11$ , *P* < 0.01

number of focal spinal T<sub>2</sub> lesions between clinical subtypes (Table 2). Diffuse spinal cord abnormalities were found mainly in secondary progressive (10 of 32) and primary progressive multiple sclerosis patients (19 of 31), while they were found in only six of 28 relapsing–remitting patients ( $\chi^2 = 11$ ; *P* < 0.01). The presence of diffuse abnormalities in the spinal cord without focal lesions was found mostly in primary progressive patients (10 of 31 patients), while it occurred in only four of 32 secondary progressive patients and in none of relapsing–remitting patients ( $\chi^2 = 15$ ; *P* < 0.01). In all patients who had diffuse spinal cord abnormalities without focal lesions, the spinal cord appeared diffusely abnormal at all vertebral levels (Fig. 3). Median spinal cord cross-sectional area was smallest in the secondary progressive group, followed by the primary progressive and relapsing–remitting groups. Patients who had diffuse spinal cord abnormalities had significantly smaller mean spinal cord cross-sectional area (67 mm<sup>2</sup>; range 49–82) than did patients with no, or only focal, abnormalities (cross-sectional area = 75 mm<sup>2</sup>; range 55–96; *P* < 0.01).

### Correlation between brain and spinal cord abnormalities

Concerning the total study population, a trend towards correlation was found between the number of focal brain T<sub>1</sub> lesions and the number of focal spinal T<sub>2</sub> lesions (*r* = 0.22; *P* < 0.05). No other correlation between brain and spinal

cord parameters was found. More specifically, no correlation was found between brain T<sub>1</sub> lesion load and spinal cord cross-sectional area, or between ventricular volume and spinal cord cross-sectional area. However, the presence of diffuse spinal cord abnormalities was associated with the presence of diffuse brain abnormalities. Ten of 35 (28.5%) patients showing diffuse spinal cord abnormalities also showed diffuse brain abnormalities. In contrast, only six of 56 (11%) patients without diffuse spinal cord abnormalities showed diffuse brain abnormalities ( $\chi^2 = 5.0$ ; *P* < 0.05). When only patients were considered who had diffuse spinal cord abnormalities without focal lesions, this association even became stronger: six of 14 (43%) patients with only diffuse spinal cord abnormalities also had diffuse brain abnormalities. In contrast, 10 of the remaining 77 patients (13%) showed diffuse brain abnormalities ( $\chi^2 = 7.1$ ; *P* = 0.015). Further, MRI parameters were correlated locally, as evidenced by correlation between brain ventricular volume and T<sub>1</sub> lesion load (*r* = 0.57; *P* < 0.000), and between the number of spinal cord segments diffusely involved and spinal cord cross-sectional area (*r* = -0.32; *P* = 0.003).

### Correlation between MRI parameters and clinical symptoms: total study population

Correlation coefficients between MRI parameters and clinical measures are summarized in Table 3. In general, brain MRI abnormalities showed trends towards correlation with scores

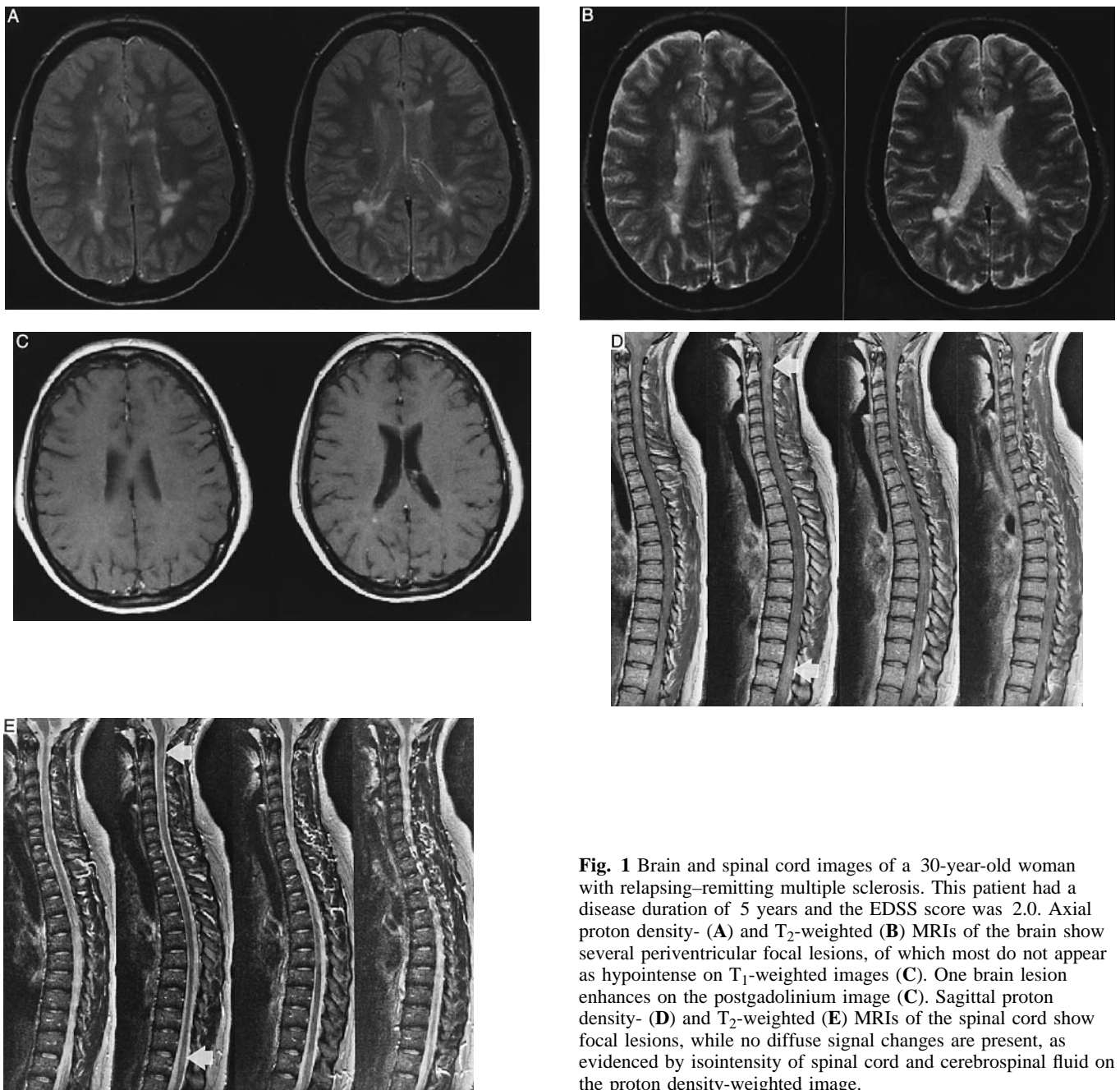


**Fig. 1** Brain and spinal cord images of a 30-year-old woman with relapsing–remitting multiple sclerosis. This patient had a disease duration of 5 years and the EDSS score was 2.0. Axial proton density- (A) and T<sub>2</sub>-weighted (B) MRIs of the brain show several periventricular focal lesions, of which most do not appear as hypointense on T<sub>1</sub>-weighted images (C). One brain lesion enhances on the postgadolinium image (C). Sagittal proton density- (D) and T<sub>2</sub>-weighted (E) MRIs of the spinal cord show focal lesions, while no diffuse signal changes are present, as evidenced by isointensity of spinal cord and cerebrospinal fluid on the proton density-weighted image.

for brain symptoms, while spinal cord MRI abnormalities correlated well with spinal cord symptoms, as illustrated by the good correlation between spinal MRI parameters and the urology complaint score. Regarding the EDSS, there were only trends towards correlation between EDSS and brain T<sub>1</sub> and T<sub>2</sub> lesion loads. By contrast, we found a good correlation between EDSS and spinal cord MRI parameters (Table 3).

Based on the correlation coefficients described above, multiple regression analysis was performed, using EDSS and the urology score as dependent variables. This yielded a model which explained 18% of EDSS variance, and which included brain T<sub>1</sub> lesion load and spinal cord cross-sectional area as factors independently contributing to EDSS (Table 4).

Using the urology score as the dependent variable, only the number of spinal cord segments diffusely involved was included in the model (Table 5).

**Correlation between MRI parameters and clinical symptoms: relapsing–remitting and secondary progressive subtypes**

Correlation coefficients between MRI parameters and clinical measures are summarized in Table 6. When considering relapsing–remitting and secondary progressive patients, the clinicoradiological correlation differed from that in the whole

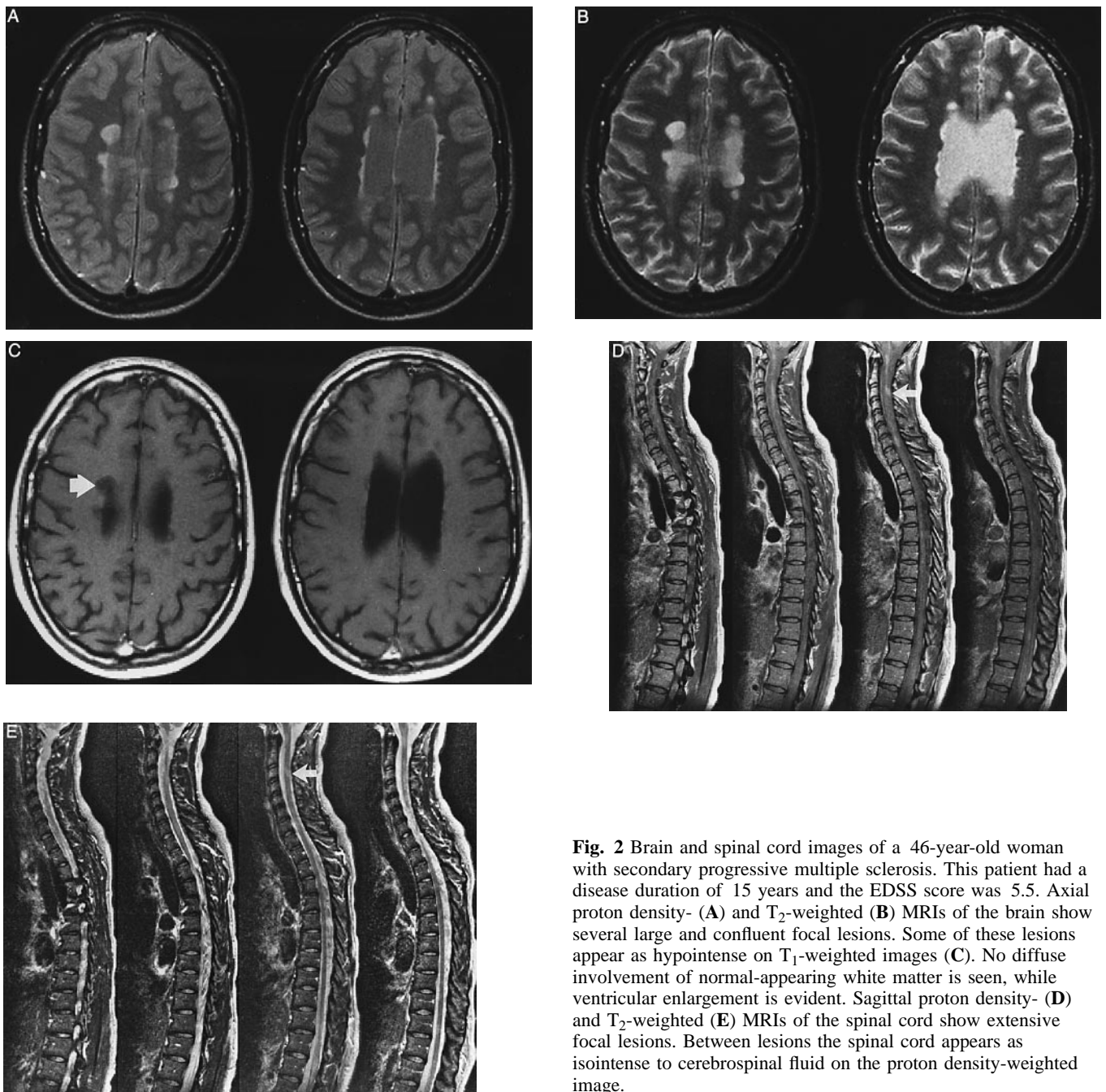


**Fig. 2** Brain and spinal cord images of a 46-year-old woman with secondary progressive multiple sclerosis. This patient had a disease duration of 15 years and the EDSS score was 5.5. Axial proton density- (A) and T<sub>2</sub>-weighted (B) MRIs of the brain show several large and confluent focal lesions. Some of these lesions appear as hypointense on T<sub>1</sub>-weighted images (C). No diffuse involvement of normal-appearing white matter is seen, while ventricular enlargement is evident. Sagittal proton density- (D) and T<sub>2</sub>-weighted (E) MRIs of the spinal cord show extensive focal lesions. Between lesions the spinal cord appears as isointense to cerebrospinal fluid on the proton density-weighted image.

study population. A correlation was found between EDSS and all brain MRI parameters, including ventricle volume (Table 6). EDSS further correlated with spinal cord cross-sectional area. FSS subscores associated with spinal cord dysfunction correlated well with spinal cord MRI parameters (Table 6). Spinal cord symptoms, however, also correlated with brain MRI parameters, as illustrated by the correlation between brain MRI parameters and the bowel/bladder FSS subscore (Table 6).

Multiple regression analysis using EDSS as the dependent variable and the parameters described above as independent variables yielded a model which explained 36% of EDSS variance, and which included brain T<sub>1</sub> lesion load, brain

ventricle volume and spinal cord cross-sectional area as factors independently contributing to EDSS (Table 4). Using the urology score as the dependent variable, the number of spinal cord segments diffusely involved and the T<sub>1</sub> lesion load in the brain were both included in the model (Table 5).

**Correlation between MRI and clinical symptoms: primary progressive subtype**

Correlation coefficients between MRI parameters and clinical measures are summarized in Table 7. None of the brain or spinal cord MRI parameters correlated with EDSS. The urology complaint score, the bowel/bladder score and the

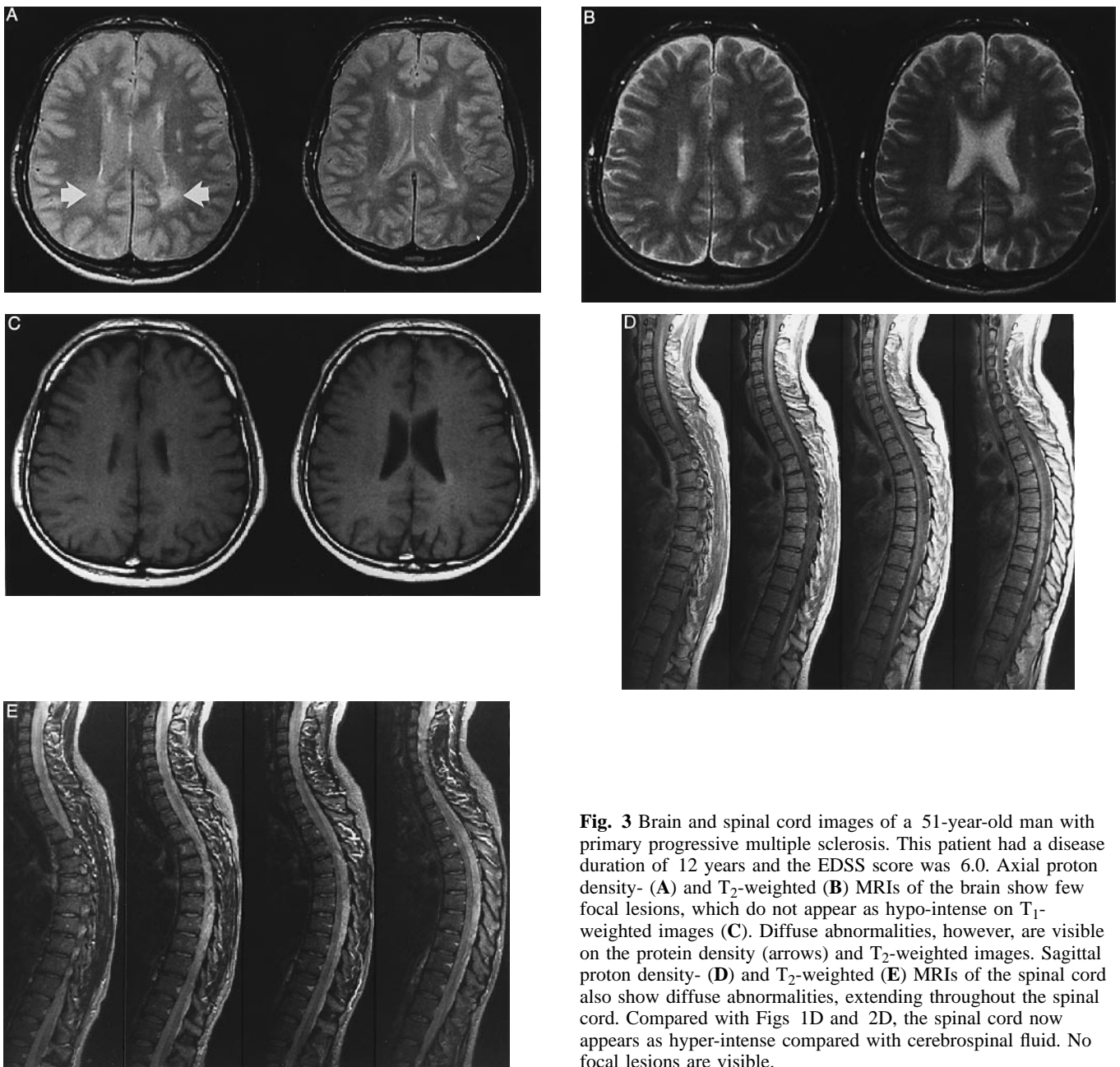


**Fig. 3** Brain and spinal cord images of a 51-year-old man with primary progressive multiple sclerosis. This patient had a disease duration of 12 years and the EDSS score was 6.0. Axial proton density- (A) and T<sub>2</sub>-weighted (B) MRIs of the brain show few focal lesions, which do not appear as hypo-intense on T<sub>1</sub>-weighted images (C). Diffuse abnormalities, however, are visible on the protein density (arrows) and T<sub>2</sub>-weighted images. Sagittal proton density- (D) and T<sub>2</sub>-weighted (E) MRIs of the spinal cord also show diffuse abnormalities, extending throughout the spinal cord. Compared with Figs 1D and 2D, the spinal cord now appears as hyper-intense compared with cerebrospinal fluid. No focal lesions are visible.

sensory score, however, showed trends towards correlation with spinal cord cross-sectional area and with the number of spinal cord segments diffusely involved.

No multiple regression model was found which could explain the variance in EDSS for the primary progressive subgroup (Table 4). Using the urology score as the dependent variable, brain T<sub>1</sub> lesion load was found to explain most of the variance in urology complaint score (Table 5).

## Discussion

From the results of this study we were able to evaluate differences between clinical subgroups in multiple sclerosis with respect to MRI parameters in the brain and spinal cord

in a large group of 91 patients. The results confirm previous studies on brain and spinal cord MRI in multiple sclerosis, which showed considerable differences between subgroups (Koopmans *et al.*, 1989; Thompson *et al.*, 1990, 1991; Kidd *et al.*, 1993).

Apart from evaluating conventional MRI parameters, we evaluated two relatively new brain MRI parameters: diffuse abnormalities and ventricular enlargement. Our method for measuring ventricular volume yielded no information about peripheral (cortical) brain atrophy or about cerebellar atrophy. However, the clear differences in ventricular volume between the subgroups and the correlation with clinical parameters suggest that our method sufficed for the purpose of this study. Regarding diffuse brain abnormalities, scoring this MRI

**Table 3** Correlations between MRI parameters and clinical data: whole study population (n = 91)

	Brain MRI parameters			Spinal cord MRI parameters		
	T <sub>1</sub> lesion load (cm <sup>3</sup> )	T <sub>2</sub> lesion load (cm <sup>3</sup> )	Ventricle volume (cm <sup>3</sup> )	T <sub>2</sub> lesion load (no. segments)	Diffuse abnormalities (no. segments)	CSA (mm <sup>2</sup> )
EDSS	0.22 (0.03)	0.21 (0.05)	–	–	0.33 (0.002)	–0.34 (0.001)
Urology score	–	–	–	–	0.44 (<0.000)	–0.30 (0.006)
FSS						
Visual	–	–	–	–	–	–
Mental	0.25 (0.02)	0.24 (0.03)	0.23 (0.04)	–	–	–
Brainstem	0.31 (0.004)	0.31 (0.004)	0.25 (0.03)	–	–	–
Cerebellar	–	–	–	–	–	–
Pyramidal	0.26 (0.02)	–	0.25 (0.03)	–	0.28 (0.01)	–0.27 (0.012)
Sensory	–	–	–	–	0.43 (<0.001)	–0.28 (0.01)
Bowel/bladder	–	–	–	–	0.43 (<0.001)	–0.43 (<0.001)

Spearman rank correlation coefficients are shown, with the P value in brackets. CSA = cross-sectional area; FSS = Functional System Score.

**Table 4** Multiple regression analysis: MRI parameters explaining disability in multiple sclerosis

Variable	Dependent variable: EDSS score			
	Coefficient	SE	Partial correlation	P
Whole study population (n = 91; r <sup>2</sup> = 0.19)				
Brain T <sub>1</sub> lesion load (cm <sup>3</sup> )	0.16	0.05	0.30	0.005
Spinal cord CSA (mm <sup>2</sup> )	–0.06	0.02	–0.29	0.005
RR and SP (n = 60; r <sup>2</sup> = 0.36)				
Brain T <sub>1</sub> lesion load (cm <sup>3</sup> )	0.15	0.06	0.30	0.011
Spinal cord CSA (mm <sup>2</sup> )	–0.06	0.02	–0.30	0.010
Brain ventricle volume (cm <sup>3</sup> )	0.04	0.02	0.26	0.025

Separate analyses were done for the total study population and either the relapsing–remitting and secondary progressive subtypes or the primary progressive subtype. SE = standard error of coefficient; CSA = cross-sectional area; RR = relapsing–remitting; SP = secondary progressive.

**Table 5** Multiple regression analysis: MRI parameters explaining urological complaints

Variable	Dependent variable: urology score			
	Coefficient	SE	Partial correlation	P
Whole study population (n = 91; r <sup>2</sup> = 0.14)				
No. spinal cord segments diffusely involved	0.28	0.06	0.46	0.000
RR and SP (n = 60; r <sup>2</sup> = 0.25)				
Brain T <sub>1</sub> lesion load (cm <sup>3</sup> )	0.34	0.12	0.33	0.009
No. spinal cord segments diffusely involved	0.20	0.08	0.33	0.01
PP subgroup (n = 31; r <sup>2</sup> = 0.22)				
Brain T <sub>1</sub> lesion load (cm <sup>3</sup> )	–0.69	0.28	–0.47	0.021

Separate analyses were done for the total study population and for either the relapsing–remitting and secondary progressive subtypes or the primary progressive subtype. SE = standard error of coefficient; RR = relapsing–remitting; SP = secondary progressive; PP = primary progressive.

parameter may be subjective. Therefore, this parameter was scored by two observers by consensus and we substantiated our findings to contrast measurements. Brain MRIs were scored only for the presence or absence of diffuse brain abnormalities. Theoretically, the quantitation of diffuse areas in the brain could be a better parameter than merely scoring the images for the presence of diffuse abnormalities. Image segmentation of diffuse abnormalities, however, is difficult

because of poor delineation of such abnormalities. Other MRI techniques, like magnetization transfer imaging (Filippi *et al.*, 1995a), histogram analysis (van Buchem *et al.*, 1996) and spectroscopy (Grossman *et al.*, 1992; Miller, 1995; Larsson, 1995; Kimura *et al.*, 1996), may provide better tools to quantitate diffuse brain abnormalities.

Based on our results and on previous studies, MRI characteristics of each subgroup are summarized in Table 8.



**Table 6** Correlations between MRI parameters and clinical data: RR and SP subgroups (*n* = 60)

	Brain MR parameters			Spinal cord MR parameters		
	T <sub>1</sub> lesion load (cm <sup>3</sup> )	T <sub>2</sub> lesion load (cm <sup>3</sup> )	Ventricle volume (cm <sup>3</sup> )	T <sub>2</sub> lesion load (no. segments)	Diffuse abnormalities (no. segments)	CSA (mm <sup>2</sup> )
EDSS	0.43 (0.001)	0.33 (0.008)	0.34 (0.007)	–	–	–0.43 (0.001)
Urology score	–	–	–	–	0.35 (0.009)	–
FSS						
Visual	–	–	–	–	–	–
Mental	0.26 (0.05)	–	0.29 (0.03)	–	–	–
Brainstem	0.38 (0.004)	0.37 (0.005)	0.35 (0.009)	–	0.32 (0.02)	–
Cerebellar	0.28 (0.03)	–	0.31 (0.02)	–	–	–0.30 (0.03)
Pyramidal	0.32 (0.016)	0.31 (0.02)	0.29 (0.03)	–	0.29 (0.03)	–0.34 (0.01)
Sensory	–	–	–	–	0.33 (0.01)	–
Bowel/bladder	0.39 (0.004)	0.33 (0.014)	0.37 (0.005)	–	0.37 (0.005)	–0.38 (0.005)

Spearman rank correlation coefficients are shown, with the *P* value in brackets. CSA = cross-sectional area; RR = relapsing–remitting; SP = secondary progressive, FSS = functional systems score.

**Table 7** Correlations between MRI parameters and clinical data: PP subgroup (*n* = 31)

	Brain MR parameters			Spinal cord MRI parameters		
	T <sub>1</sub> lesion load (cm <sup>3</sup> )	T <sub>2</sub> lesion load (cm <sup>3</sup> )	Ventricle volume (cm <sup>3</sup> )	T <sub>2</sub> lesion load (no. segments)	Diffuse abnormalities (no. segments)	CSA (mm <sup>2</sup> )
EDSS	–	–	–	–	–	–
Urology score	–	–	–	–	0.39 (0.047)	–0.39 (0.05)
FSS						
Visual	–	–	–	–	–	–
Mental	–	–	–	–	–	–
Brainstem	–	–	–	–	–	–
Cerebellar	–	–	–	–	–	–
Pyramidal	–	–	0.45 (0.02)	–	–	–
Sensory	–	–	–	–	0.47 (0.01)	–0.39 (0.04)
Bowel/bladder	–	–	–	–0.39 (0.04)	0.42 (0.03)	–0.41 (0.04)

Spearman rank correlation coefficients are shown, with the *P* value in brackets. CSA = cross-sectional area; RR = relapsing–remitting; SP = secondary progressive; FSS = functional systems score.

**Table 8** Summary of MRI imaging findings in clinical subgroups of multiple sclerosis

	Relapsing–remitting	Secondary progressive	Primary progressive
Brain			
Focal T <sub>2</sub> lesions	many	many	few
Occurrence of enhancing lesions	often	often	seldom
Focal T <sub>1</sub> lesions	few	many	few
Patients with diffuse abnormalities	seldom	variable	typical
Ventricular volume enlargement	seldom	typical	seldom
Spinal cord			
Focal T <sub>2</sub> lesions variable	many	few	
Focal T <sub>1</sub> lesions	never	never	never
Patients with diffuse abnormalities	seldom	variable	typical
Spinal cord atrophy	seldom	typical	typical

Relapsing–remitting multiple sclerosis differs mostly from other subgroups by the relative absence of diffuse abnormalities and of atrophy. Secondary progressive multiple sclerosis may be differentiated from the other subgroups by a larger proportion of brain lesions appearing as hypo-intense

on T<sub>1</sub>-weighted MRIs, and by atrophy of both the brain and the spinal cord. Primary progressive patients often have diffuse abnormalities in the brain and spinal cord, while they often have only a few focal lesions despite a high degree of disability.

### **Relationship between brain and spinal cord abnormalities**

Spinal cord atrophy and diffuse signal increase may reflect secondary changes caused by brain abnormalities, as has been reported to occur in Wallerian degeneration (Sawhani *et al.*, 1997). Our results did not substantiate this theory in multiple sclerosis patients, since these spinal cord MRI abnormalities were not related either to the focal brain lesion load or to ventricular enlargement. Spinal cord abnormalities, however, followed the same pattern in the brain, as indicated by the simultaneous occurrence of diffuse abnormalities in the brain and spinal cord. This suggests that all spinal cord abnormalities found represented local pathology and were not secondary to brain abnormalities.

### **Relationship between MRI appearance and clinical scores**

Since relapsing–remitting and secondary progressive multiple sclerosis may be considered as two phases of the same disease and primary progressive multiple sclerosis may be a separate entity (McDonnell and Hawkins, 1996), we performed our analysis with respect to these subgroups. The higher EDSS scores in secondary progressive patients compared with relapsing–remitting patients were determined to a large extent by spinal cord symptoms. In agreement with this finding, multiple regression analysis revealed independent contributions to EDSS by both brain and spinal cord MRI parameters. This illustrates the usefulness of integrating MRI of the brain and spinal cord in attempts to explain disability in multiple sclerosis.

In the primary progressive subgroup spinal cord MRI parameters correlated well with spinal cord symptoms, illustrating the importance of spinal cord involvement in primary progressive multiple sclerosis. None of the MRI parameters, however, could explain EDSS in primary progressive multiple sclerosis. This may have been caused by lack of variance in EDSS in this group. Alternatively, current MRI methods may not represent the full extent of the disease process. Since we did not quantitate the amount of diffuse brain involvement we may have underestimated the amount of brain abnormalities. New techniques for the quantitation of generalized brain involvement in multiple sclerosis, such as magnetization transfer histogram analysis and spectroscopy (Loevner *et al.*, 1995; van Buchem *et al.*, 1996), may improve the clinicoradiological correlation in primary progressive multiple sclerosis. Also, these new MRI methods may further improve the clinicoradiological correlation in relapsing–remitting and secondary progressive multiple sclerosis, since our combined parameters still explained only 36% of EDSS variance in these subtypes.

In conclusion, the integration of MRI findings for the brain and spinal cord indicates that different clinical courses may be associated with distinct MRI patterns in multiple sclerosis.

In relapsing–remitting and secondary progressive multiple sclerosis, disability can be explained at least partly by features revealed by the currently available MRI techniques. Brain abnormalities seem to explain most of the symptoms and disability in these subtypes, while in primary progressive multiple sclerosis spinal cord abnormalities seem to be clinically more important than brain abnormalities. Finally, our results indicate that brain and spinal cord abnormalities may develop independently of each other in multiple sclerosis.

### **Acknowledgements**

We wish to thank Arno Kuiper for helping with quantitation of brain abnormalities. Dr Lycklama à Nijeholt is funded by the Dutch Multiple Sclerosis Society (grant 92–131).

### **References**

- Aschoff JC, Lindner U, Kornhuber HH. Demyelination foci and brain atrophy in the cranial computer tomogram in multiple sclerosis. [German]. *Nervenarzt* 1984; 55: 208–13.
- Filippi M, Barker GJ, Horsfield MA, Sacares PR, MacManus DG, Thompson AJ. Benign and secondary progressive multiple sclerosis: a preliminary quantitative MRI study. *J Neurol* 1994; 241: 246–51.
- Filippi M, Campi A, Dousset V, Baratti C, Martinelli V, Canal N, et al. A magnetization transfer imaging study of normal-appearing white matter in multiple sclerosis. *Neurology* 1995a; 45: 478–82.
- Filippi M, Paty DW, Kappos L, Barkhof F, Compston DA, Thompson AJ, et al. Correlations between changes in disability and T<sub>2</sub>-weighted brain MRI activity in multiple sclerosis: a follow-up study. *Neurology* 1995b; 45: 255–60.
- Filippi M, Campi A, Colombo B, Pereira C, Martinelli V, Baratti C, et al. A spinal cord MRI study of benign and secondary progressive multiple sclerosis. *J Neurol* 1996; 243: 502–5.
- Gasparini C, Horsfield MA, Thorpe JW, Kidd D, Barker GJ, Tofts PS, et al. Macroscopic and microscopic assessments of disease burden by MRI in multiple sclerosis: relationship to clinical parameters. *J Magn Reson Imaging* 1996; 6: 580–4.
- Grossman RI, Lenkinski RE, Ramer KN, Gonzalez-Scarano F, Cohen JA. MRI proton spectroscopy in multiple sclerosis. *Am J Neuroradiol* 1992; 13: 1535–43.
- Kidd D, Thorpe JW, Thompson AJ, Kendall BE, Mosely IF, MacManus DG, et al. Spinal cord MRI using multi-array coils and fast spin echo. II. Findings in multiple sclerosis. *Neurology* 1993; 43: 2632–7.
- Kidd D, Thorpe JW, Kendall BE, Barker GJ, Miller DH, McDonald WI, et al. MRI dynamics of brain and spinal cord in progressive multiple sclerosis. *J Neurol Neurosurg Psychiatry* 1996; 60: 15–9.
- Kimura H, Grossman RI, Lenkinski RE, Gonzalez-Scarano F. Proton MRI spectroscopy and magnetization transfer ratio in multiple sclerosis: correlative findings of active versus irreversible plaque disease. *Am J Neuroradiol* 1996; 17: 1539–47.
- Koopmans RA, Li DK, Grochowski E, Cutler PJ, Paty DW. Benign

versus chronic progressive multiple sclerosis: magnetic resonance imaging features. *Ann Neurol* 1989; 25: 74–81.

Kurtzke JF. On the evaluation of disability in multiple sclerosis. *Neurology* 1961; 11: 686–94.

Kurtzke JF. Rating neurologic impairment in multiple sclerosis: an expanded disability status scale (EDSS). *Neurology* 1983; 33: 1444–52.

Larsson HB. In vivo characterization of the multiple sclerosis plaque by magnetic resonance imaging and spectroscopy. *Acta Neurol Scand* 1995; Suppl 159: 1–44.

Loevner LA, Grossman RI, Cohen JA, Lexa FJ, Kessler D, Kolson DL. Microscopic disease in normal-appearing white matter on conventional MRIs in patients with multiple sclerosis: assessment with magnetization-transfer measurements. *Radiology* 1995; 196: 511–5.

Losseff NA, Webb SL, O’Riordan JI, Page R, Wang L, Barker GJ, et al. Spinal cord atrophy and disability in multiple sclerosis. A new reproducible and sensitive MRI method with potential to monitor disease progression. *Brain* 1996a; 119: 701–8.

Losseff NA, Wang L, Lai HM, Yoo DS, Gawnw-Cain ML, McDonald WI, et al. Progressive cerebral atrophy in multiple sclerosis. A serial MRI study. *Brain* 1996b; 119: 2009–19.

Lycklama à Nijeholt GJ, Barkhof F, Scheltens P, Castelijns JA, Ader H, van Waesberghe JH, et al. MRI of the spinal cord in multiple sclerosis: relation to clinical subtype and disability. *AJNR Am J Neuroradiol* 1997; 18: 1041–8.

McDonnell GV, Hawkins SA. Primary progressive multiple sclerosis: a distinct syndrome? *Multiple Sclerosis* 1996; 2: 137–41.

Miller DH. Magnetic resonance imaging and spectroscopy in multiple sclerosis. [Review]. *Curr Opin Neurol* 1995; 8: 210–5.

Miller DH, Albert PS, Barkhof F, Francis G, Frank JA, Hodgkinson S, et al. Guidelines for the use of magnetic resonance techniques in monitoring the treatment of multiple sclerosis. *Ann Neurol* 1996; 39: 6–16.

Sawlani VG, Gupta RK, Singh MK, Kohli A. MRI Demonstration of Wallerian degeneration in various intracranial lesions and its clinical implications. *J Neurol Sci* 1997; 146: 103–8.

Thompson AJ, Kermode AG, MacManus DG, Kendall BE, Kingsley DP, Moseley IF, et al. Patterns of disease activity in multiple sclerosis: clinical and magnetic resonance imaging study [see comments]. *BMJ* 1990; 300: 631–634. Comment in: *BMJ* 1990; 300: 1272.

Thompson AJ, Kermode AG, Wicks D, MacManus DG, Kendall BE, Kingsley DP, et al. Major differences in the dynamics of primary and secondary progressive multiple sclerosis. *Ann Neurol* 1991; 29: 53–62.

Thorpe JW, Kidd D, Moseley IF, Kendall BE, Thompson AJ, MacManus DG, et al. Serial gadolinium-enhanced MRI of the brain and spinal cord in early relapsing–remitting multiple sclerosis. *Neurology* 1996; 46: 373–8.

Truyen L, van Waesberghe JH, van Walderveen MA, van Oosten BW, Polman CH, Hommes OR, et al. Accumulation of hypointense

lesions (‘black holes’) on T<sub>1</sub> spin-echo MRI correlates with disease progression in multiple sclerosis. *Neurology* 1996; 47: 1469–76.

van Buchem MA, McGowan JC, Kolson DL, Polansky M, Grossman RI. Quantitative volumetric magnetization transfer analysis in multiple sclerosis: estimation of macroscopic and microscopic disease burden. *Magn Reson Med* 1996; 36: 632–6.

van Walderveen MA, Barkhof F, Hommes OR, Polman CH, Tobi H, Frequin ST, et al. Correlating MRI and clinical disease activity in multiple sclerosis: relevance of hypointense lesions on short-TR/short-TE (T<sub>1</sub>-weighted) spin-echo images. *Neurology* 1995; 45: 1684–90.

Received August 15, 1997. Revised October 17, 1997

Accepted November 21, 1997

## Appendix 1. Urological complaints questionnaire

### Irritative complaints

#### Urge complaints

0 = no complaints; 1 = few complaints; 2 = moderately many complaints; 3 = serious complaints

#### Nycturia (frequency)

0 = 0–1 times each night; 2 = twice each night; 3 = three times each night; 4 = four or more times per night

#### Miction frequency during the day

0 = less than every 3 hours; 1 = every 2–3 hours; 2 = every 1–2 hours; 3 = more than once per hour

#### Pain during miction

0 = never; 1 = sometimes; 2 = rather often; 3 = serious pain

### Obstructive complaints

#### Quality of urine jet

0 = normal; 1 = variable; 2 = weak; 3 = dripping

#### Pushing during miction

0 = no; 1 = yes

#### Residue feeling after miction

0 = no; 1 = yes

#### Difficulties starting miction

0 = no; 1 = yes

#### Halting of miction

0 = no; 1 = yes

### Incontinence complaints

#### Incontinence when increasing abdominal pressure

0 = no; 1 = yes

#### Does urination start automatically?

0 = yes; 1 = sometimes yes, sometimes no; 2 = no

#### Urge incontinence

0 = no; 1 = yes

### Urinary tract infections

#### Regularly complaining of urinary tract infection

0 = no; 1 = less than twice each year; 2 = more than twice each year

### Sexual problems

#### Impotence, loss of feeling

0 = no; 1 = yes